Information exchange dynamics of the two-dimensional XY model

Minsu Kim,[1,2] Daun Jeong,[3] H. W. Kwon,[1,4] and M. Y. Choi[1,*]

[1]*Department of Physics and Astronomy and Center for Theoretical Physics, Seoul National University, Seoul 151-747, Korea*

[2]*Soil and Terrestrial Environmental Physics (STEP), Institute of Terrestrial Ecosystems (ITES), ETH Zurich, 8092 Zurich, Switzerland*

[3]*Computational Science Group, Samsung Advanced Institute of Technology, Yongin 446-712, Korea*

[4]*School of Physics, Korea Institute for Advanced Study, Seoul 130-722, Korea*

(Received 23 August 2013; revised manuscript received 7 October 2013; published 25 November 2013)

Information exchange dynamics of the two-dimensional XY model is studied by means of the entropic sampling algorithm. Combining the analytic and numerical results, we obtain the entropy in the whole range of the energy at various system sizes. The time evolution of the order parameter and of the number of vortices is explored, and the corresponding relaxation times are found to grow algebraically with the system size. Such absence of characteristic time scales in the thermodynamic limit manifests the emergent criticality of the exchanging process of information with the environment. The mechanism of information exchange in the XY model is discussed in terms of the dynamic exponents, in comparison with the Ising model.

DOI: 10.1103/PhysRevE.88.052134 PACS number(s): 05.40.−a, 05.65.+b, 75.10.Hk, 89.75.Fb

I. INTRODUCTION

The importance of the role of entropy in the biological evolution has been addressed in literature [1]. In general, every species attempts to minimize its entropy, obtaining information from the environment. By applying this concept, it has been shown that the biological evolution of an ecosystem can be adequately described by the information exchange dynamics employing the entropic sampling algorithm [2]. Over the past few years, simulations based on entropic sampling have been performed, primarily focusing on the globally coupled and the two-dimensional Ising model [3,4]. Those results can be related to a wide range of phenomena in biological and social systems [5,6]. Furthermore, such dynamics has been recognized as an adequate theoretical explanation of the reason why scale invariance is observed so common in nature. In this respect, the ubiquity of the emergent dynamical criticality is expected regardless of the details of the system, as long as the dynamics is directed by information exchange to and from the environment.

The XY model has often been used for the description of physical, biological, and social systems in which the states of individual constituents are specified by phase variables and interactions between the constituents depend on the corresponding phase differences [7,8]. This model, particularly in two dimensions, is well known for its characteristics such as quasi-long-range order, vortex pairs, and the Berezinski-Kosterlitz-Thouless (BKT) transition [9], and has been extensively studied over the past few decades. However, the entropy or the density of states has not been fully determined yet although several studies have addressed the density of states [10]. Further, there is no inherent dynamics of this model, and appropriate dynamics should be specified, depending on the system it models.

In this study, we investigate the information exchange dynamics in the two-dimensional XY model. The information exchange between the system and environment is realized with the entropic sampling dynamics, which is subject to the exact estimation of the entropy for the entire range of the energy. It has been a challenge to obtain the entropy of the XY model, possessing the continuous U(1) symmetry. We first evaluate the entropy by means of the entropic sampling algorithm, supplemented by analytic results in the immediate vicinity of the ground state. Using the obtained entropy, we perform entropic sampling Monte Carlo (MC) simulations, which corresponds to the information exchange dynamics.

This paper is organized as follows: Sec. II is devoted to the entropy of the two-dimensional XY model. The entropy of the system is obtained numerically in the whole range of the energy. Moreover, at high and low temperatures, analytic expressions of the entropy are given as functions of the energy. In Sec. III, information exchange dynamics of the system is investigated by means of the entropic sampling algorithm, and corresponding numerical results are presented. We estimate the relaxation time from the time correlation functions of the order parameter and the number of vortices and compute the dynamic exponents as well. Finally, Sec. IV gives a summary.

II. ENTROPY OF THE TWO-DIMENSIONAL XY MODEL

In this section we present the entropy of the system. At general temperatures the entropy is computed through the use of Monte Carlo simulations, employing the entropic sampling algorithm. In addition, analytic expressions are also obtained in the low- and high-temperature limits.

The two-dimensional XY model is described by the Hamiltonian

$$\mathcal{H} = -J \sum_{\langle i,j \rangle} \cos(\theta_i - \theta_j), \tag{1}$$

where θ_i is the phase angle of the ith spin and $\langle i,j \rangle$ denotes the nearest-neighboring pairs. There are $N (= L^2)$ spins, forming an $L \times L$ square lattice. Henceforth, for simplicity, the coupling strength will be set equal to unity ($J \equiv 1$). From Eq. (1), the partition function of the system obtains the form

$$\mathcal{Z} = \int \left(\prod_i \frac{d\theta_i}{2\pi} \right) \exp\left[\beta \sum_{\langle i,j \rangle} \cos(\theta_i - \theta_j) \right], \tag{2}$$

*mychoi@snu.ac.kr

where β is the inverse temperature (with the Boltzmann constant set to be unity: $k_B \equiv 1$).

A. Numerical estimation

The continuous U(1) symmetry makes it formidable to study numerically the XY model. It is usually the case that the XY model is approximated as a clock model with the (discrete) Z_q symmetry. Namely, the phase angle θ_i is made discrete and replaced by $2\pi p_i/q$ with p_i taking an integer between 1 and q. This results in the q-state clock model, described by the Hamiltonian

$$\mathcal{H} = -J \sum_{\langle i,j \rangle} \cos\left[\frac{2\pi}{q}(p_i - p_j)\right]. \tag{3}$$

When $q > 4$, this model is known to exhibit two transitions, although the interpretation of the data and the locations of the transitions raise rather a subtle problem [11]. In particular, as q is increased, the lower transition temperature approaches zero while the transition at the higher transition temperature corresponds to the BKT transition in the XY model. This indeed demonstrates that the q-state clock model reduces to the XY model in the limit $q \to \infty$, and it is thereby possible to adopt the clock model with large q as an approximation to the XY model. In this study, we choose $q = 60$, which turns out large enough to yield essentially the same results as the continuous model and is numerically tractable in the entropic sampling algorithm.

To obtain the entropy $S(e)$ as a function of the energy per spin $e\,(\equiv E/N)$, we follow the steps in Ref. [12]: Beginning with a random configuration, we get a rough estimate of $S(e)$, which is initially set to be zero for all e. We then obtain the histogram $H(e)$ from MC sweeps satisfying the detailed balance condition

$$\frac{w(\vec{\sigma}\to\vec{\sigma}')}{w(\vec{\sigma}'\to\vec{\sigma})} = e^{-\Delta S}, \tag{4}$$

where $w(\vec{\sigma}\to\vec{\sigma}')$ is the transition rate from configuration $\vec{\sigma} \equiv \{\sigma_1,\sigma_2,\ldots,\sigma_N\}$ to $\vec{\sigma}' \equiv \{\sigma_1',\sigma_2',\ldots,\sigma_N'\}$, and $\Delta S \equiv S[e(\vec{\sigma}')] - S[e(\vec{\sigma})]$ is the change in the entropy. Specifically, a trial update from $\vec{\sigma}$ to $\vec{\sigma}'$ is accepted with the probability $p = \min\{1, e^{-\Delta S}\}$. After the first iteration, which is effectively random sampling of 10^4 MC sweeps [recall $S(e)$ is zero at this stage], we raise $S(e)$ by the amount $\ln H(e)$ for $H(e) \neq 0$. The next iteration then starts from the new estimate of $S(e)$. Subsequently, we perform 8×10^6 MC sweeps to obtain a new histogram and update $S(e)$ by adding $\ln H(e)$. The range of the sampled energy increases with the number of iterations. The iteration is repeated until the entire energy space is sampled uniformly and $S(e)$ thus remains unchanged up to an additive constant.

In order to obtain $S(e)$ properly, one should choose carefully the width of the energy bin for the histogram. Since the entropy is ideally a continuous function of the energy, it is desirable to use a narrow bin: If the bin width is too large compared with the typical change of the energy density in an MC update, the energy would not be uniformly sampled. On the other hand, too small width would result in poor numerical convergence. In this work, we choose 2.00×10^{-3} (in unit of J) for the bin width of the energy density.

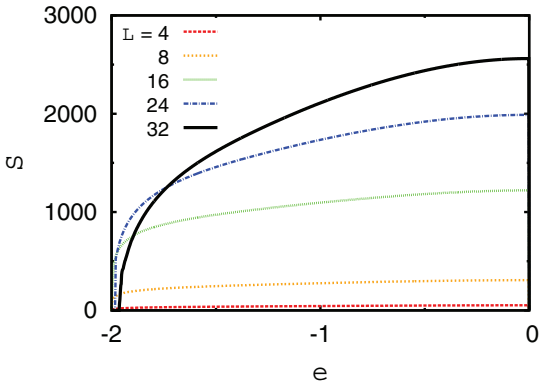

FIG. 1. (Color online) Total entropy S as a function of the energy (per spin) e, obtained numerically for various system sizes.

Figure 1 shows the entropy of the XY model, obtained as a function of the energy, for $L = 4,8,16,24$, and 32. Note that $S(e)$ increases monotonically with e, which reflects that the system possesses more accessible states at higher energies, thus leading to the disordered state. In contrast, low-energy states are progressively less accessible, especially at large system sizes such as $L = 24$ and 32, because the total number of accessible states grows exponentially with the system size. To overcome this and to attain proper sampling, we increase the number of MC sweeps and iterations in the low-energy region, to the best of our computing capability.

The detailed result for $L = 32$ in the energy range $-2.0 < e < -1.6$, shown in Fig. 2, manifests insufficient sampling in the low-energy region; this appears inevitable, making it necessary to employ other methods. As an alternative algorithm, the microcanonical MC technique may be promising in the low-energy region [13]. Here, for convenience, we use the analytic result in the low-temperature limit, where the low-energy states are expected to prevail at equilibrium; this is discussed in the next subsection.

B. Analytical expressions

We next consider analytical expressions of the entropy in the two temperature limits, low- and high-temperature limits. At

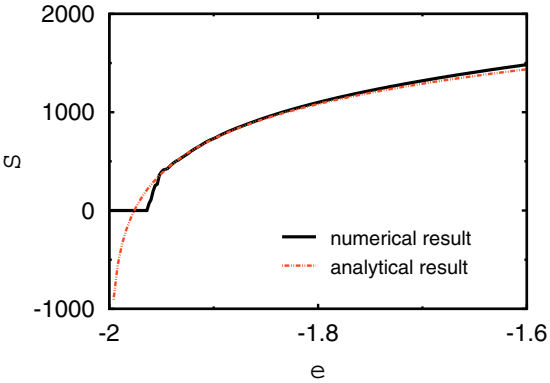

FIG. 2. (Color online) Total entropy $S(e)$ in the low-energy region, obtained numerically for $L = 32$ (black solid line) in comparison with the analytical result $S_{sw}(e) - S_0$ (red dashed line) given by Eq. (5).

low temperatures the state of the system is close to the ground state, which makes the spin-wave approximation applicable. This leads to the entropy as a function of the energy per spin $e\,(\equiv E/N)$:

$$S_{\rm sw}(e) = \frac{N-3}{2}\ln(e+2) + \frac{N-3}{2}\ln N + S_0, \qquad (5)$$

which is accurate in the vicinity of the ground state [10]. $s \equiv S_{\rm sw}/N$ with $S_{\rm sw}$ given by Eq. (5), Here it is convenient to adjust the additive constant S_0 in such a way that the entropy vanishes at the lowest off-ground-state energy $e = e_0$, which is set equal to -1.998.

As displayed in Fig. 2, the analytic result agrees reasonably well with the numerical result over a considerable range of e. This presumably reflects that fluctuations of configurations sampled numerically belong mostly to the regime where the spin-wave approximation is valid. Accordingly, we can extrapolate the numerically obtained entropy, with the help of the analytic expression, to the low-energy region. In this manner, the entropy could be determined up to the lowest off-ground-state energy $e_0 = -1.998$ in our analysis.

At high temperatures, we expand Eq. (2) in terms of powers of β and obtain

$$\begin{aligned}\mathcal{Z} &\approx 1 + \frac{1}{2}\beta^2 \int \prod_i \frac{d\theta_i}{2\pi}\left[\sum_{\langle i,j\rangle}\cos(\theta_i-\theta_j)\right]^2 + O(\beta^4)\\ &= 1 + \frac{1}{2}N\beta^2 + O(\beta^4), \qquad (6)\end{aligned}$$

where it has been noted that the terms of odd powers of the cosine function vanish. From the partition function, it is straightforward to obtain the entropy in the form

$$S \approx -1 + \sqrt{1-2Ne^2} + \ln\left(\frac{1-\sqrt{1-2Ne^2}}{Ne^2}\right), \qquad (7)$$

which is accurate in the vicinity of $e = 0$, i.e., in the limit of small β. Note that the entropy here, obtained from differentiation of the partition function, takes apparently negative values; adding an appropriate constant yields the true (positive) values.

Analytical results in the high- and low-energy regions are observed to be consistent with the numerical results presented in Sec. II A. Combining numerical and analytical results, we obtain the entropy of the system in the entire range of the energy e, which is presented in Fig. 3. The results for $L = 4,8,16$ are obtained solely by numerical simulations. Here the additive constant has been adjusted, so that the value of the entropy coincides at $e = e_0$ regardless of the system size.

Naturally, the entropy of the XY model is an increasing function of the energy, similar to that of the Ising model [4]. Compared with the Ising model, however, the entropy increases more rapidly in the low-energy region, which results from the fact that the number of possible states increases explosively. (Note the sharp contrast that each spin in the Ising model can assume only two states.) In addition, the entropy can also be obtained efficiently through the use of the Wang-Landau histogram method and our result is also consistent with that in Ref. [10].

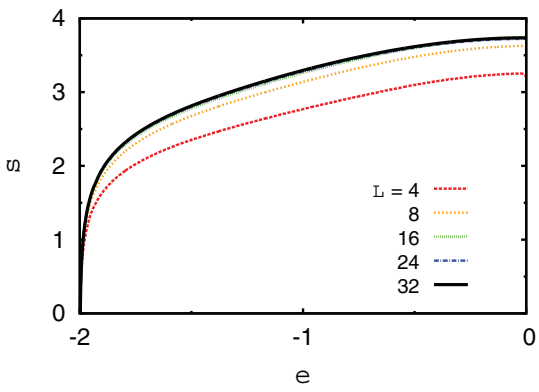

FIG. 3. (Color online) Entropy (per spin) s as a function of the energy (per spin) e for various system sizes. Curves for different system sizes have been shifted appropriately, by adjusting the constant S_0 for each system size, to set $s(e = -1.998) \equiv 0$.

III. ENTROPIC SAMPLING DYNAMICS

In this section, we examine information exchange dynamics via extensive MC simulations employing the entropic sampling algorithm. As in the preceding numerical steps obtaining the entropy, the phase angle of a randomly chosen spin is updated to one of q discrete angles with the probability $p = \min\{1, e^{-\Delta S}\}$, where S is the entropy obtained in Sec. II. The transitions among the microscopic states are then controlled by the entropy, and elements in this ensemble are distributed according to $e^{-S[e(\vec{\sigma})]}$. Of particular interest is the dynamics of the order parameter and vortices, with a view to characterizing the process of information exchange in the XY model. The unit of time in MC simulations is set equal to one sweep of the updating procedure for all N spins in the system.

A. Dynamics of the order parameter

Ordering in the system can be described with the order parameter m, defined to be

$$m \equiv \frac{1}{N}\sqrt{\left(\sum_i^N \cos\theta_i\right)^2 + \left(\sum_i^N \sin\theta_i\right)^2}. \qquad (8)$$

When m vanishes, the spins are randomly oriented; m approaches unity as the spins are aligned in one direction. The order parameter m evolves with time t, and we probe how it evolves in the entropic sampling dynamics.

Figure 4 displays the typical behavior of $m(t)$ for $L = 4,8,16$, and 32 in the time range $4\,000 \leqslant t \leqslant 16\,000$. The dynamics of a smaller system is observed to be faster in general and to cover a wider range of m. Two small systems of size $L = 4$ and 8 tend to prefer relatively ordered states ($m > 0.5$): m increases immediately after reaching $m = 0$. In contrast, the largest system studied here ($L = 32$) exhibits slow relaxation and remains disordered. Such difference arises from the system size dependence of the entropy, as explained in Sec. II A. As L is increased, $S(e)$ becomes relatively steep in the high-energy region, which results in that the larger system is likely to stay longer in the disordered state. If a large system falls into the low-energy region where m is close to unity, the present state

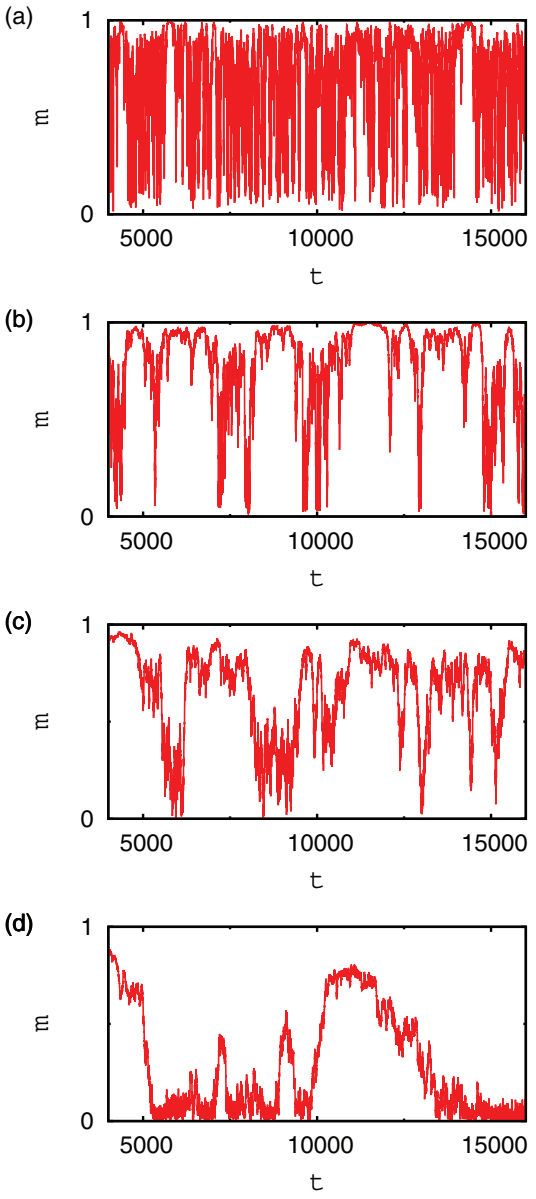

FIG. 4. (Color online) Time evolution of the order parameter m for the system size $L =$ (a) 4, (b) 8, (c) 16, and (d) 32.

may then persist because the entropy is now too steep for the system to reach the disordered state easily.

In general, the time evolution of a system is conveniently characterized by the relaxation of autocorrelations. We thus define the normalized time correlation function of the order parameter:

$$C(t) \equiv \frac{\langle m(t)m(0)\rangle - \langle m(t)\rangle^2}{\langle m^2(0)\rangle - \langle m(0)\rangle^2}, \tag{9}$$

where $\langle\cdots\rangle$ denotes the ensemble average. In practice, assuming ergodicity and stationarity in the entropic sampling dynamics, we take the time average over t' in the expression $\langle m(t+t')m(t')\rangle_{t'}$; this is meant by $\langle m(t)m(0)\rangle$. The time correlation function $C(t)$, obtained for various system sizes, is shown in Fig. 5. As noticed in the semilogarithmic plot, $C(t)$ exhibits nonexponential decay for all system sizes. Moreover, the relaxation of $C(t)$ becomes slower as L is increased.

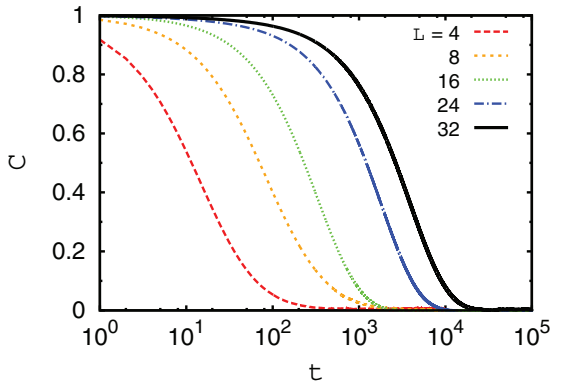

FIG. 5. (Color online) Evolution of the time correlation function $C(t)$ of the order parameter m for various system sizes.

To probe the relaxation in the thermodynamic limit, we consider the relaxation time τ defined to be the integration of the normalized time correlation function:

$$\tau \equiv \int_0^\infty dt\ C(t). \tag{10}$$

Figure 6(a) presents the relaxation time τ, obtained for various system sizes. It is observed that τ grows algebraically with the

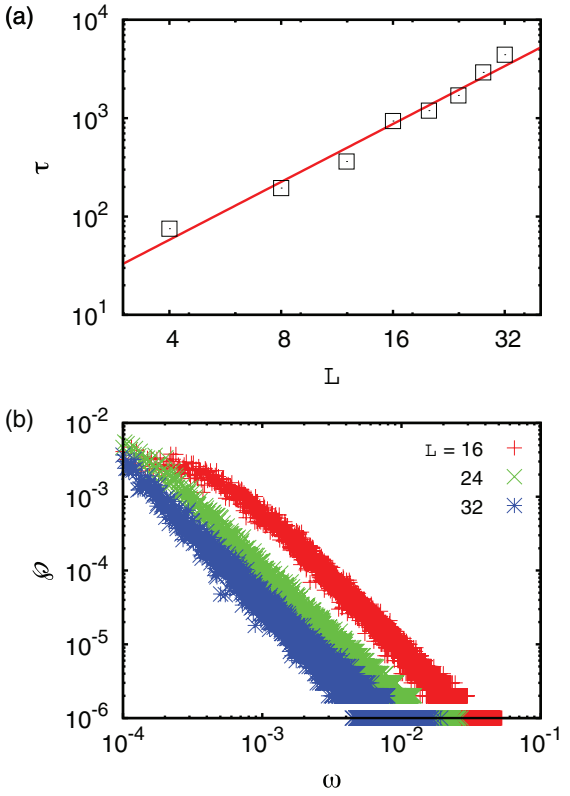

FIG. 6. (Color online) (a) Relaxation time τ (in units of the MC sweep per spin) versus the system size L on the logarithmic scale. Squares represent data points, fitted to the straight line of the slope 1.96. (b) Power spectrum $\mathcal{P}$ as a function of frequency ω, obtained from the Fourier transform of the correlation function $C(t)$ for several system sizes, on the logarithmic scale.

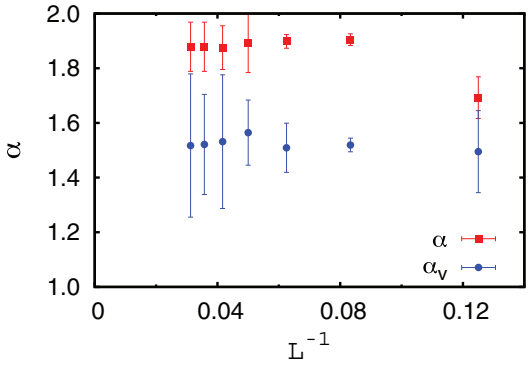

FIG. 7. (Color online) The power spectrum exponent α versus the inverse size L^{-1}. Blue squares and red circles represent data points for the power spectra of the order parameter and of vortices. Error bars have been estimated from the data dispersion in Figs. 6(b) and 9(b).

system size L:

$$\tau \sim L^z, \tag{11}$$

with the dynamic exponent $z = 1.96 \pm 0.12$. We also present in Fig. 6(b) the power spectrum $\mathcal{P}(\omega)$ of the order parameter m for $L = 16$, 24, and 32, which apparently exhibits the power-law behavior, $\mathcal{P}(\omega) \sim \omega^{-\alpha}$. The frequency range in which the power-law behavior persists extends with L, demonstrating the emergence of critical behavior in the thermodynamic limit. To obtain the exponent α, we carry out the finite-size scaling analysis with the help of Fig. 7, which exhibits α versus the inverse system size L^{-1}. This yields the estimation $\alpha \approx 1.88 \pm 0.09$.

The absence of the characteristic time scale in the thermodynamic limit can be interpreted as the criticality of the entropic sampling dynamics. In particular, the nontrivial value of the dynamic exponent z would not be reproduced by simple rescaling of the time steps of simulations for larger systems. This indicates that the observed criticality should be an emergent property arising from cooperativity of the information exchange in the system, possibly suggesting the general mechanism for self-organized criticality [3,14]. In comparison with the two-dimensional Ising model [3], of which the dynamic exponent in the entropic sampling dynamics is known as $z \approx 2.6$, the two-dimensional XY model displays faster dynamics. It is of interest that the time scale of the entropic sampling dynamics can generally be understood in terms of the entropic barriers of the system [15,16]. The exponent of the power spectrum of the order parameter, $\alpha \approx 1.88$, appears smaller than the exponent for the globally coupled Ising model and the two-dimensional Ising model ($\alpha = 2$) [3]. The entropy of the XY model increases more rapidly than that of the Ising model in the low-energy region, as addressed in Sec. II A. Such enhanced entropic barriers would result in slower relaxation. On the contrary, however, our result reveals that the relaxation is faster. In the light of the dynamics of the model, sampling in the low-energy region is not liable to encounter in a large system because of the behavior of the entropy. Thus inferred is the existence of other information exchange processes besides the spin ordering. Specifically, in the two-dimensional XY model, contributions of vortex dynamics can be significant, as discussed in Sec. III B.

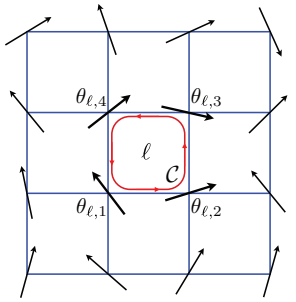

FIG. 8. (Color online) Diagram for calculating the number of vortices.

B. Dynamics of vortices

In this section, we examine the contributions of vortices in the information exchange dynamics of the two-dimensional XY model. Considering the time evolution of the total number N_v of vortices, we compute its relaxation time τ_v from the time correlation function of N_v for various system sizes. First, the charge of a vortex at face l on the lattice is obtained as follows: Along the closed path $\mathcal{C}$ around the face l, the vortex charge is given by

$$n_l = \frac{1}{2\pi} \sum_{a=1}^{4} [(\theta_{l,a+1} - \theta_{l,a}) (\mathrm{mod}\, 2\pi)], \tag{12}$$

where the summation index a labels the position on the closed path $\mathcal{C}$ around the face l (see Fig. 8). Thus, the position labeled by $a = 5$ is identified with that by $a = 1$. The total number N_v of vortices in the system is defined to be the sum of the number of vortices with positive charge ($n_l > 0$) and the number of vortices with negative charge ($n_l < 0$). In the calculation, vortices with unit charge ($n_l = \pm 1$) turn out to be dominant and those with charge larger than unity are rarely observed. Furthermore, because of the pair creation-annihilation of vortices, both the number of vortices with charge $+1$ and the number with negative charge -1 show essentially the same behavior as the total number N_v. From the obtained results of the time evolution of $N_v(t)$, the time correlation function and the relaxation time are obtained in the same manner as those of the order parameter in Eqs. (9) and (10).

Figures 9(a) and 9(b) display the relaxation time of vortex dynamics versus the system size L and the power spectrum $\mathcal{P}_v(\omega)$ of the total vortex number $N_v(t)$, respectively. The relaxation time τ_v is observed to grow algebraically with the size, obeying $\tau_v \sim L^z$ with the dynamic exponent $z = 2.78 \pm 0.12$. Note that the dynamic exponent for N_v is larger than that for the order parameter, indicating that dynamics of vortices exhibits critical behavior more progressively as the thermodynamic limit is approached. The configurational entropy related to the formation of vortices would play an important role in the information dynamics. In the low-energy region, the configurational entropy increases logarithmically with the system size; this contributes to the information exchange dynamics of the system and produces the observed criticality. Demonstrated in Fig. 9(b) is the power-law behavior of the power spectrum: $\mathcal{P}_v(\omega) \sim \omega^{-\alpha_v}$, where the exponent estimated from Fig. 7 is given by $\alpha_v = 1.5 \pm 0.2$.

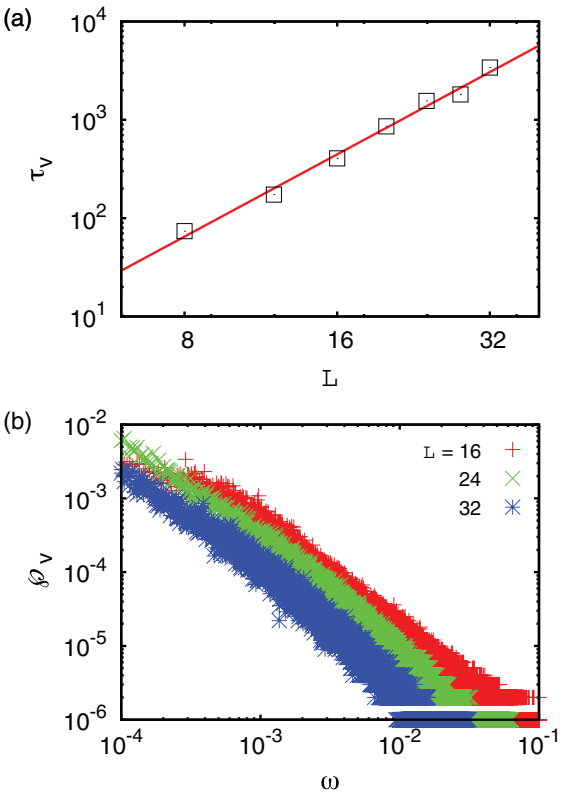

FIG. 9. (Color online) (a) Relaxation time τ_v (in units of the MC sweep per spin) of the vortex number versus the system size L. Squares represent data points, fitted to the straight line of the slope 2.78. (b) Power spectrum $\mathcal{P}_v(\omega)$ of the vortex number, obtained from the Fourier transform of the correlation function of $N_v(t)$ for several system sizes.

IV. CONCLUSION

Information exchange dynamics of the two-dimensional XY model has been studied via MC simulations. We have first computed the entropy of the system numerically and analytically. Analytic expressions for the entropy, obtained in the high- and low-temperature limits have been found to agree well with the numerical results obtained via the entropic sampling algorithm. Then numerical simulations of the information exchange dynamics of a two-dimensional XY model is carried out through the use of the entropic sampling algorithm, which is based on the reversible information exchange with the environment. When the system encounters with information acquisition during entropic fluctuations, the dynamics proceeds to reduce the entropy followed by relaxation thereafter. From the time evolution of the order parameter, we have obtained the time correlation function and the relaxation time depending on the system size. The algebraic growth of the relaxation time with the size manifests criticality of the entropic sampling dynamics in the thermodynamic limit, characterized by the nontrivial dynamic exponent $z \approx 1.96$. Further, the power spectrum of the order parameter turns out to exhibit power-law behavior, with the exponent $\alpha \approx 1.88$. Interestingly, the dynamic exponent is smaller than that for the Ising model, despite that this model possesses more prominent entropic barriers in the low-energy region. Recall that the system of size $L = 32$ becomes hardly ordered, as observed in the time evolution of the order parameter. We expect that the information exchange is not probed solely by spin ordering dynamics, considering not only the continuous symmetry of the spin variables but also the absence of long-range order in equilibrium.

In view of this, we have also examined the dynamics of vortices with regard to the evolution of the number of vortices. It has been found that the corresponding dynamic exponent takes the value $z_v \approx 2.78$, substantially larger than that for the order parameter. This indicates the importance of the vortex motion in the critical dynamics of information exchange.

ACKNOWLEDGMENTS

This work was supported by National Research Foundation of Korea through the Basic Science Research Program (Grants No. 2012R1A2A4A01004419 and No. 2011-0012331).

[1] W. Ebeling and R. Feistel, J. Non-Equilib. Thermodyn. **17**, 303 (1992).
[2] M. Y. Choi, H. Y. Lee, D. Kim, and S. H. Park, J. Phys. A **30**, L749 (1997).
[3] M. Y. Choi, B. J. Kim, B.-G. Yoon, and H. Park, Europhys. Lett. **69**, 503 (2005).
[4] B. J. Kim and M. Y. Choi, J. Phys. A **38**, 2115 (2005).
[5] M. Kuperman and D. Zanette, Eur. Phys. J. B **26**, 387 (2002).
[6] P. Babinec, Phys. Lett. A **225**, 179 (1997).
[7] T. Vicsek, A. Czirok, E. Ben-Jacob, I. Cohen, and O. Shochet, Phys. Rev. Lett. **75**, 1226 (1995); J. Toner and Y. Tu, *ibid*. **75**, 4326 (1995).
[8] H. Y. Lee and M. Kardar, Phys. Rev. E **64**, 056113 (2001); C. M. Bordogna and E. V. Albano, *ibid*. **76**, 061125 (2007).
[9] J. M. Kosterlitz and D. J. Thouless, J. Phys. C **6**, 1181 (1973).
[10] J. Xu and H.-R. Ma, Phys. Rev. E **75**, 041115 (2007).
[11] M. S. S. Challa and D. P. Landau, Phys. Rev. B **33**, 437 (1986).
[12] J. Lee, Phys. Rev. Lett. **71**, 211 (1993); J. Lee and M. Y. Choi, Phys. Rev. E **50**, R651 (1994).
[13] K.-C. Lee, J. Phys. A **23**, 2087 (1990); S. Lee and K.-C. Lee, Phys. Rev. B **49**, 15184 (1994).
[14] J. Kertesz and L. B. Kiss, J. Phys. A **23**, L433 (1990); E. Bonabreau and P. Lederer, *ibid*. **27**, L243 (1994).
[15] F. Ritort, Phys. Rev. Lett. **75**, 1190 (1995).
[16] B. J. Kim, G. S. Jeon, and M. Y. Choi, Phys. Rev. Lett. **76**, 4648 (1996).